Morphologically Controlled Growth of Aluminum Nitride Nanostructures by the Carbothermal Reduction and Nitridation Method

Woo-Sik Jung

School of Display and Chemical Engineering, College of Engineering, Yeungnam University, Gyongsan 712-749, Korea
E-mail: wsjung@yu.ac.kr
Received February 20, 2009, Accepted May 25, 2009

One-dimensional aluminum nitride (AlN) nanostructures were synthesized by calcining an Al(OH)(succinate) complex, which contained a very small amount of iron as a catalyst, under a mixed gas flow of nitrogen and CO (1 vol%). The complex decomposed into a homogeneous mixture of alumina and carbon at the molecular level, resulting in the lowering of the formation temperature of the AlN nanostructures. The morphology of the nanostructures such as nanocone, nanoneedle, nanowire, and nanobamboo was controlled by varying the reaction conditions, including the reaction atmosphere, reaction temperature, duration time, and ramping rate. Iron droplets were observed on the tips of the AlN nanostructures, strongly supporting that the nanostructures grow through the vapor-liquid-solid mechanism. The variation in the morphology of the nanostructures was well explained in terms of the relationship between the diffusion rate of AlN vapor into the iron droplets and the growth rate of the nanostructures.

Key Words: AlN, Nanostructures, VLS mechanism

Introduction

Aluminum nitride (AlN) has many attractive thermo-mechanical and electronic properties, such as excellent thermal conductivity, high electrical resistivity, high mechanical strength, and high melting point.[1] In addition, it has been well established that AlN has a very small and even negative electron affinity[2] which favors field emission. Accordingly, one-dimensional (1D) nanostructures of AlN are expected to be worthy field emission candidates since the 1D geometry effectively increases the enhancement factor that is essential for the turn-on field and high current density required for field emission.[3] Various 1D AlN nanostructures such as nanowhiskers,[4] nanowires,[5,6] nanocones,[7-9] naonotubes,[10-12] and nanobelts[13] have been synthesized mainly by the direct niridation method in which metallic aluminum reacts with ammonia and/or N_2.

AlN whiskers have been obtained by the carbothermal reduction and nitridation (CRN) method.[14-17] Their thickness is expected to become thinner by lowering the formation temperature of AlN.[14] The temperature is much lower in the modified CRN (mCRN) method than in the conventional CRN (cCRN) method.[18] Al(III) complexes and alumina are used as precursors in the mCRN and cCRN methods, respectively. In the present work, we show that the morphology of 1D AlN nanostructures can be controlled using the mCRN method and propose their growth mechanism. The precursor complex used in this study was Al(OH)(succinate) (hereafter referred to as AS).[18] Up to now, there have been no reports dealing with the detailed growth mechanism of 1D AlN nanostructures grown by the CRN method. Very recently we reported the characteristics of AlN nanowhiskers synthesized by mCRN method.[19]

Experimental Section

The AS complex was synthesized as described previously.[18] In this study a small amount (mole ratio of Al^{3+} to Fe^{3+} = 1 : 0.01) of iron(III) nitrate was added in synthesis of the AS complex. Hereafter, the AS complex synthesized in this study will be referred to as the Fe/AS complex. The Fe/AS powder, on the top of which (0001) sapphire was placed, was calcined without mixing it with any carbon source in an alumina crucible, which was put in an alumina tube with an inner diameter of 36 mm. The ramping rate, unless otherwise stated, was 5 °C/min and the gas flow rate was 200 mL/min. In this study, a mixture of N_2 and CO (1 vol%) gases (hereafter referred to as CO(1)/N_2) was used.

The product powders were characterized by powder X-ray diffraction (XRD) with a DMX-2500 diffractometer (Rigaku, Japan) with Cu-Kα radiation operating at 40 kV and 100 mA. The morphology and structure of the AlN products grown on the sapphire were investigated by scanning electron microscopy (SEM, Hitachi S-4100), transmission electron microscopy (TEM, Philips CM 200 STEM, working at 200 kV), and selected-area electron diffraction (SAED).

Results

Figure 1 shows XRD patterns of samples obtained by calcining the AS complex for at various temperatures for 5 h. The XRD patterns were more refined than those we previously reported[18] because of the use of higher purity (> 99.999%) N_2 gas. As shown in Figure 1(a), the sample obtained at 1100 °C exhibited only the peaks assigned to γ-Al_2O_3 (JCPDS No. 10-0425). In the sample calcined at 1150 °C, weak diffraction peaks assigned to AlN (JCPDS No. 25-1133) were detected

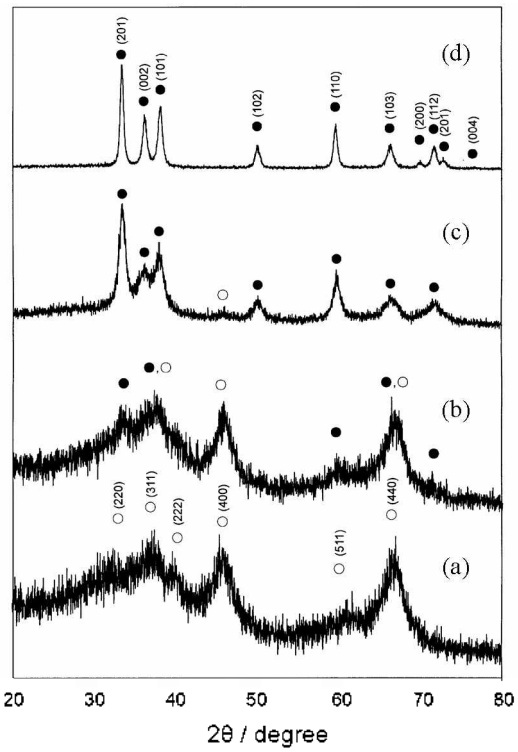

Figure 1. XRD patterns of samples obtained by calcination of (hydroxo)(succinato)aluminum(III) complex at (a) 1100, (b) 1150, (c) 1200, and (d) 1300 °C for 5 h under a flow of N_2. (●) AlN, (○) γ-Al_2O_3.

together with those assigned to γ-Al_2O_3. The sample obtained at 1200 °C exhibited intense peaks assigned to AlN together with a weak (400) peak of unreacted γ-Al_2O_3. The sample calcined at 1300 °C contained no detectable peaks other than those assigned to AlN, as shown in Figure 1(d). No AlN nanostructures were formed from the AS powder which did not contain Fe, rather these nanostructures were prepared on sapphire by calcining the Fe/AS powder under a flow of N_2 and CO(1)/N_2. In our previous paper[14] we showed that Fe_2O_3, which is derived by the pyrolysis of an Fe(III) complex, is reduced to Fe by CO evolved by the following CRN reaction.

$$Al_2O_3\,(s) + 3C(s) + N_2(g) \rightarrow 2\,AlN(s) + 3\,CO(g) \qquad (1)$$

The amount of CO evolved by the CRN reaction was not sufficient to reduce the Fe_2O_3 formed by calcining the Fe/AS powder and therefore CO was intentionally supplied into the reaction system.

Effect of the reaction atmosphere. The effect of the reaction atmosphere on the morphology of the AlN nanostructures was investigated by calcining the Fe/AS powder at 1200 °C for 5 h under flows of N_2 and CO(1)/N_2. As shown in Figures 2(a) and 2(b), AlN nanostructures with irregular and needle-like morphologies were observed under flows of N_2 and CO(1)/N_2, respectively. This morphological difference indicates that the atmosphere of CO(1)/N_2 is favorable for the growth of AlN nanostructures with a regular and distinct morphology. It is noted that the CO has a retardation effect on the CRN reaction of Al_2O_3 to AlN.[20]

The alternative supply of CO(1)/N_2 and Ar for 10 minutes each at 1200 °C yielded bamboo-like nanostructures, as shown in Figure 2(c). The stem (~ 1 μm) between two nodes in the nanostructure is thought to grow in the 10-minute period during which CO(1)/N_2 is supplied.

Effect of the reaction temperature and duration time. The AlN nanostructures were synthesized under a flow of CO(1)/N_2 in the temperature range from 1150 to 1300 °C. As shown in Figures 2(d) and 2(b), nanocones and nanoneedles with round cross sections were synthesized at 1150 and 1200 °C for 5 h, respectively. At reaction temperatures ≥ 1250 °C, nanostructures with irregular morphologies were observed, but had no Fe droplets on their tips because of the volatilization. The nanostructures (Figure 3(a)) obtained by using a temperature profile in which the temperature was gradually raised from 1000 to 1200 °C over a period of 1 h and then held at 1200 °C for 2 h shows that along the growth direction the thickness of the nanostructure linearly increased with raising the temperature from 1000 to 1200 °C and then remained constant during soaking at 1200 °C. This result indicates that

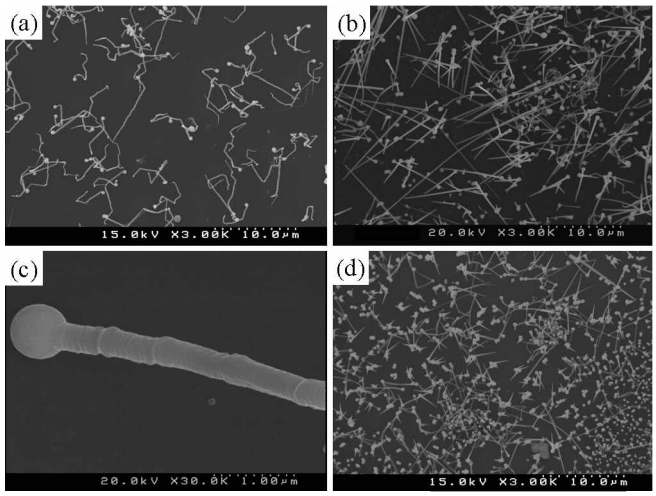

Figure 2. SEM images of AlN nanostructures obtained by calcination of Fe/AS powder under the following calcination conditions:(a) N_2 flow at 1200 °C for 5 h; (b) CO(1)/N_2 flow at 1200 °C for 5 h; (c) an alternative flow of CO(1)/N_2 and Ar for 10 minute each at 1200 °C; (d) CO(1)/N_2 flow at 1150 °C for 5 h. The CO(1)/N_2 means a mixed gas of N_2 and CO (1 vol%).

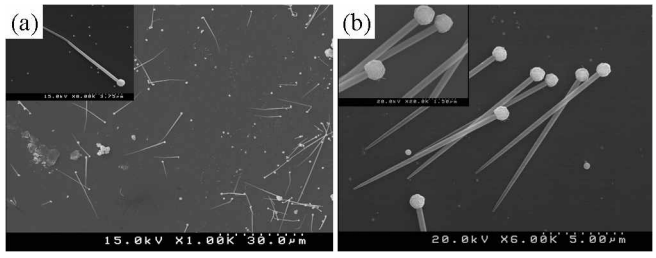

Figure 3. SEM images of AlN nanostructures obtained by calcination of Fe/AS powder under a flow of CO(1)/N_2 using the following temperature profiles: (a) the temperature was raised from 1000 to 1200 °C over a period of 1 h and then held at 1200 °C for 2 h; (b) the ramping rate was 1 °C/min and the powder was soaked at 1100 °C for 2 h, 1150 °C for 2 h, and then 1200 °C for 2 h.

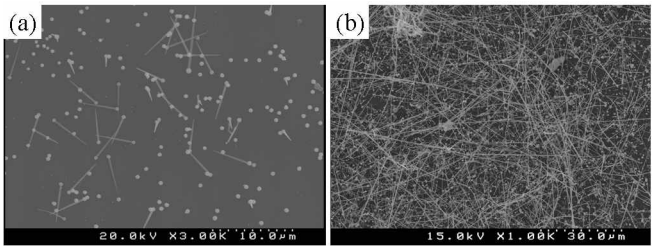

Figure 4. SEM images of AlN nanostructures obtained by calcination of Fe/AS powder under a flow of CO(1)/N_2 at 1200 °C for (a) 1 and (b) 15 h.

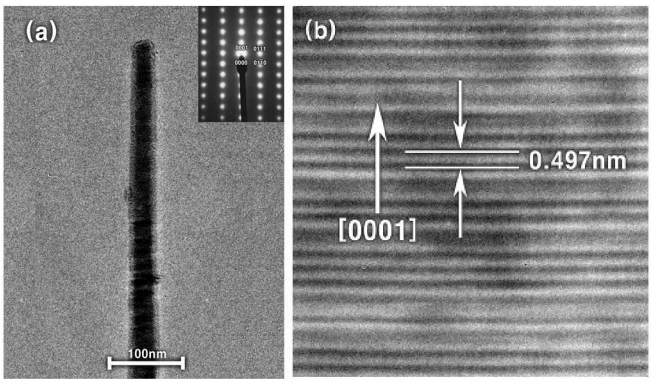

Figure 5. (a) TEM image of an AlN nanoneedle. The inset shows the SAED pattern, with the zone axis being [$2\bar{1}\bar{1}0$]. (b) HRTEM image of a single crystalline AlN nanoneedle, with the preferential growth direction being [0001].

the thickness of the nanoneedles increases with increasing reaction temperature.[14]

Increasing the duration time caused the length of the nanostructures to be increased. For example, the nanostructures (Figure 4(a)) obtained by calcination at 1200 °C for 1 h were nanocones with a length of 5 to 6 μm, while the nanostructures (Figure 4(b)) obtained by calcination at 1200 °C for 15 h were nanowires with a length of several hundreds μm. These nanostructures are compared with the nanoneedles (Figure 2 (b)) obtained by calcination at 1200 °C for 5 h.

Effect of the ramping rate. The ramping rate of the temperature also had an effect on the morphology of the nanostructures. Ramping rates of 1 and 5 °C/min yielded nanoneedles with hexagonal and round cross sections, respectively. For example, Figure 3(b) shows the nanoneedles with a hexagonal cross section. They were obtained using a temperature profile in which the ramping rate was 1 °C/min and the precursor was soaked at 1100 °C for 2 h, 1150 °C for 2 h, and then 1200 °C for 2 h.

TEM image of AlN nanoneedles. TEM and high-resolution TEM (HRTEM) images, along with selected-area electron diffraction (SAED) pattern were measured to characterize the structure of nanoneedles. Figure 5(a) shows that a typical AlN nanoneedle has a sharp tip of 30 nm. As demonstrated in the corresponding HRTEM image (Figure 5(b)), the nanoneedle is a single crystal with a distance of 0.497 nm between the adjacent lattice planes, in agreement with d_{0001} space of wurtzite AlN, confirming that the preferred growth direction of the nanoneedle is [0001].[7-9]

Discussion

Growth mechanism of AlN nanostructures. All of the nanostructures obtained at the temperature ≤ 1200 °C carry nanosized (200 to 700 nm) droplets on their tips, strongly suggesting that they grow via the vapor-liquid-solid (VLS) mechanism.[21] The energy-dispersive X-ray spectroscopic measurements revealed that the droplets consisted of Fe.[15] These Fe droplets, which are derived by the reduction of Fe_2O_3 by CO and then evaporation, act as a catalyst in the VLS mechanism. The melting point of nanosized Fe droplets is expected to be much lower than that (1536 °C) of bulk Fe. On the basis of these results, we suggest the growth mechanism as follows: when AlN vapor diffuses into an Fe droplet, the droplet becomes supersaturated and an AlN seed subsequently precipitates from it. The continuous diffusion of AlN vapor into the droplet sustains the axial and radial growth of the AlN seed, resulting in the formation of AlN nanostructures. The increase in the length with the duration time is ascribed to the axial growth in a direction of [0001], while the increase in the thickness with the reaction temperature is ascribed to the radial growth.

The variation in the morphology of the AlN nanostructures is well explained in terms of the relationship between the diffusion rate of AlN vapor into the Fe droplets and the growth rate of the nanostructures. When the former rate surpasses the latter one, the nanostructure has an irregular morphology. This is the case for the reaction system in which the Fe/AS powder is calcined under a flow of pure N_2 gas (Figure 2(a)) or under a flow of CO(1)/N_2 above 1250 °C. This irregular morphology may be caused by the formation of low-crystallinity AlN seeds in the Fe droplets. The low crystallinity may be due to the time insufficient for the AlN seeds to become crystalline because of the high diffusion rate of AlN vapor into the Fe droplet. The formation and diffusion rates of AlN vapor in the CO(1)/N_2 atmosphere are expected to be lower than those in the N_2 atmosphere because of the retardation effect of CO in the CRN reaction,[20] and are suitable for the continuous growth of single-crystal AlN nanostructures such as nanocones and nanoneedles. If the ramping rate decreases, both the diffusion rate of AlN vapor and the growth rate of AlN seed slowly increase. Therefore, the lowering of the ramping rate causes the AlN seeds to be much more highly crystalline, resulting in the growth of AlN nanoneedles with a hexagonal cross section (Figure 3(b)).

Formation mechanism of tapered tips. The thickness of the nanoneedles grown via the VLS mechanism increased with increasing the reaction temperature, indicating that the tapered tip of the nanostructures is formed as the reaction temperature is reached.[19] It seems, therefore, that the existence of the tapered tip also constitutes evidence for the VLS mechanism. The thickness of the AlN whiskers grown by the cCRN method was micrometer-sized because of high growth temperature (~ 1800 °C).[15-17] The whiskers did not carry any catalytic droplets, the existence of which is characteristic of the VLS

mechanism, but it seems to be reasonable to assume that they also grew *via* the VLS mechanism because most of them had tapered tips.

Liu *et al.*[7] prepared AlN nanocones on metal-coated Si wafers by the reaction of NH_3 with $AlCl_3$ and suggested that they grow through the vapor-liquid mechanism. They assumed that the formation of nanocones could be ascribed to a progressive decrease in the amount of the AlN species along the axial growth direction.

Conclusions

This study has demonstrated that the mCRN method is a useful method to synthesize various 1D AlN nanostructures at relatively low reaction temperatures. The morphology of the nanostructures was controlled by varying the reaction conditions, including the reaction atmosphere, reaction temperature, duration time, and ramping rate. These nanostructures were grown *via* the VLS mechanism, in which AlN vapor diffuses into the Fe droplets. The variation in the morphology of the nanostructures was well explained in terms of the relationship between the diffusion rate of AlN vapor into the iron droplets and the growth rate of the nanostructures. The thickness of the 1D nanostructures increased with increasing reaction temperature, indicating that the tapered tip of the nanostructures is formed as the reaction temperature is reached.

Acknowledgments. This work was supported by the National Center for Nanomaterials Technology through Yeungnam University in 2008. The SEM and TEM images were recorded at the Yeungnam University Instrumental Analysis Center.

References

1. Sheppard, L. M. *Am. Ceram. Soc. Bull.* **1990**, *31*, 1801.
2. Wu, C. I.; Kahn, A.; Hellmann, E. S.; Buchanan, D. N. *Appl. Phys. Lett.* **1998**, *73*, 1346.
3. Bonard, J. M.; Kind, H.; Stockli, A. T.; Nilsson, L. O. *Solid-State Electron.* **2001**, *45*, 893.
4. Haber, J. A.; Gibbons, P. C.; Buhro, W. E. *Chem. Mater.* **1998**, *10*, 4062.
5. Zhang, Y.; Liu, J.; He, R.; Zhang, Q.; Zhang, X.; Zhu, J. *Chem. Mater.* **2001**, *13*, 3899.
6. Wu, Q.; Hu, Z.; Wang, X.; Lu, Y.; Huo, K.; Deng, S.; Xu, N.; Shen, B.; Zhang, R.; Chen, Y. *J. Mater. Chem.* **2003**, *13*, 2024.
7. Liu, C.; Hu, Z.; Wu, Q.; Wang, X.; Chen, Y.; Sang, H.; Zhu, J.; Deng, S.; Xu, N. *J. Am. Chem. Soc.* **2005**, *127*, 1318.
8. Shi, S.-C.; Chen, C.-F.; Chattopadhyay, S.; Lan, Z.-H.; Chen, K.-H.; Chen, L.-C. *Adv. Func. Mater.* **2005**, *15*, 781.
9. Shi, S.-C.; Chattopadhyay, S.; Chen, C.-F.; Chen, K.-H.; Chen, L.-C. *Chem. Phys. Lett.* **2006**, *418*, 152.
10. Tondare, V. N.; Balasubramanian, C.; Shene, S. V.; Joag, D. S.; Godbole, V. P.; Bhoraskra, S. V. *Appl. Phys. Lett.* **2002**, *80*, 4813.
11. Wu, Q.; Hu, Z.; Wang, X.; Lu, Y.; Chen, X.; Xu, H.; Chen, Y. *J. Am. Chem. Soc.* **2003**, *125*, 10176.
12. Yin, L.-W.; Bando, Y.; Zhu, Y.-C.; Li, M.-S.; Tang, C.-C.; Golberg, D. *Adv. Mater.* **2005**, *17*, 213.
13. Wu, Q.; Hu, Z.; Wang, X.; Chen, Y.; Lu, Y. *J. Phys. Chem. B* **2003**, *107*, 9726.
14. Jung, W.-S.; Joo, H. U. *J. Crystal Growth* **2005**, *285*, 566.
15. Caceres, P. G.; Schmid, H. K. *J. Am. Ceram. Soc.* **1994**, *77*, 977.
16. Miao, W.-G.; Wu, Y.; Zhou, H.-P. *J. Mater. Sci.* **1997**, *32*, 1969.
17. Fu, R.; Zhou, H.; Chen, L.; Wu, Y. *Mater. Sci. Eng. A* **1999**, *266*, 44.
18. Jung, W.-S.; Ahn, S.-K. *J. Mater. Chem.* **1994**, *4*, 949.
19. Jung, W.-S.; Joo, H. U. *Physica E* **2008**, *40*, 833.
20. Joo, H. U.; Jung, W.-S. *J. Mater. Proc. Technol.* **2008**, *204*, 498.
21. Wagner, R. S.; Ellis, W. C. *Appl. Phys. Lett.* **1964**, *4*, 89.